Critical appraisal of technologies to assess electrical activity during atrial fibrillation: a position paper from the European Heart Rhythm Association and European Society of Cardiology Working Group on eCardiology in collaboration with the Heart Rhythm Society, Asia Pacific Heart Rhythm Society, Latin American Heart Rhythm Society and Computing in Cardiology

Natasja M.S. de Groot[1]*, **Dipen Shah**[2], **Patrick M. Boyle**[3], **Elad Anter**[4], **Gari D. Clifford**[5], **Isabel Deisenhofer**[6], **Thomas Deneke**[7], **Pascal van Dessel**[8], **Olaf Doessel**[9], **Polychronis Dilaveris**[10], **Frank R. Heinzel**[11], **Suraj Kapa**[12], **Pier D. Lambiase**[13], **Joost Lumens**[14], **Pyotr G. Platonov**[15], **Tachapong Ngarmukos**[16], **Juan Pablo Martinez**[17], **Alejandro Olaya Sanchez**[18], **Yoshihide Takahashi**[19], **Bruno P. Valdigem**[20], **Alle-Jan van der Veen**[21], **Kevin Vernooy**[22], **Ruben Casado-Arroyo (co-chair)**[23]

ESC Scientific Document Group: Tom De Potter[24], Borislav Dinov[25], Jedrzej Kosiuk[26], Dominik Linz[27], Lis Neubeck[28], Emma Svennberg[29,30], Young-Hoon Kim[31], Elaine Wan[32], Nestor Lopez-Cabanillas[33,34], Emanuela T. Locati[35], and Peter Macfarlane[36]

[1]Department of Cardiology, Erasmus University Medical Centre, Rotterdam, Delft University of Technology, Delft the Netherlands; [2]Cardiology Service, University Hospitals Geneva, Geneva, Switzerland; [3]Department of Bioengineering, University of Washington, Seattle, Washington, USA; [4]Cardiac Electrophysiology Section, Department of Cardiovascular Medicine, Cleveland Clinic, Cleveland, Ohio, USA; [5]Department of Biomedical Informatics, Emory University, Department of Biomedical Engineering, Georgia Institute of Technology and Emory University, Atlanta, USA; [6]Department of Electrophysiology, German Heart Center Munich and Technical University of Munich, Munich, Germany; [7]Department of Cardiology, Rhon-klinikum Campus Bad Neustadt, Germany; [8]Department of Cardiology, Medisch Spectrum Twente, Twente, the Netherlands; [9]Karlsruher Institut für Technologie (KIT), Karlsruhe, Germany; [10]1st University Department of Cardiology, National & Kapodistrian University of Athens School of Medicine, Hippokration Hospital, Athens, Greece; [11]Department of Internal Medicine and Cardiology, Charité-Universitätsmedizin Berlin, Campus Virchow-Klinikum and DZHK (German Centre for Cardiovascular Research), Berlin, Germany; [12]Department of Cardiology, Mayo Clinic, Rochester, USA; [13]Barts Heart Centre and University College, London, UK; [14]Cardiovascular Research Institute Maastricht (CARIM) Maastricht University, Maastricht, the Netherlands; [15]Department of Cardiology, Clinical Sciences, Lund University, Lund, Sweden; [16]Faculty of Medicine Ramathibodi Hospital, Mahidol University, Bangkok, Thailand; [17]Aragon Institute of Engineering Research/IIS-Aragon and University of Zaragoza, Zaragoza, Spain, CIBER Bioengineering, Biomaterials and Nanomedicine (CIBER-BBN), Zaragoza, Spain; [18]Department of Cardiology, Hospital San José, Fundacion Universitaia de Ciencas de la Salud, Bogota, Colombia; [19]Department of Cardiovascular Medicine, Tokyo Medical and Dental University, Tokyo, Japan; [20]Department of Cardiology, Hospital Rede D'or São Luiz, hospital Albert einstein and Dante pazzanese heart institute, São Paulo, Brasil; [21]Department Circuits and Systems, Delft University of Technology, Delft, the Netherlands; [22]Department of Cardiology, Cardiovascular Research Institute Maastricht (CARIM), Maastricht University Medical Centre, Maastricht, the Netherlands; [23]Department of Cardiology, Erasme University Hospital, Université Libre de Bruxelles, Brussels, Belgium; [24]Cardiology Department, Olv Aalst, Aalst, Belgium; [25]Rhythmology Unit, Herzzentrum Leipzig, Leipzig, Germany; [26]Department of Electrophysiology, Helios Clinic Koethen, Koethen, Germany; [27]MUMC, Maastricht Hart en Vaat Centrum,

* Corresponding author. Tel: 010 703 39 38. *E-mail address:* n.m.s.degroot@erasmusmc.nl

Maastricht, The Netherlands; [28]Edinburgh Napier University, Edinburgh, UK; [29]Cardiology Department, Karolinska University Hospital, Sweden; [30]Department of Clinical Sciences, Danderyd's Hospital, Danderyd, Sweden; [31]Cardiology Department, Korea University Medical Center, Seoul, Republic of Korea; [32]Columbia University, New York, USA; [33]Adventist Cardiovascular Institute of Buenos Aires, Argentina; [34]Medical School, 8 College Road, Singapore; [35]Department of Arrhythmology and Electrophysiology, IRCCS Policlinico San Donato, San Donato Milanese, Milan, Italy; and [36]Electrocardiology Group, Institute of Health and Wellbeing, University of Glasgow, Level 1, New Lister Building, Royal Infirmary, Glasgow, UK

Abstract   We aim to provide a critical appraisal of basic concepts underlying signal recording and processing technologies applied for (i) atrial fibrillation (AF) mapping to unravel AF mechanisms and/or identifying target sites for AF therapy and (ii) AF detection, to optimize usage of technologies, stimulate research aimed at closing knowledge gaps, and developing ideal AF recording and processing technologies. Recording and processing techniques for assessment of electrical activity during AF essential for diagnosis and guiding ablative therapy including body surface electrocardiograms (ECG) and endo- or epicardial electrograms (EGM) are evaluated. Discussion of (i) differences in uni-, bi-, and multi-polar (omnipolar/Laplacian) recording modes, (ii) impact of recording technologies on EGM morphology, (iii) global or local mapping using various types of EGM involving signal processing techniques including isochronal-, voltage- fractionation-, dipole density-, and rotor mapping, enabling derivation of parameters like atrial rate, entropy, conduction velocity/direction, (iv) value of epicardial and optical mapping, (v) AF detection by cardiac implantable electronic devices containing various detection algorithms applicable to stored EGMs, (vi) contribution of machine learning (ML) to further improvement of signals processing technologies. Recording and processing of EGM (or ECG) are the cornerstones of (body surface) mapping of AF. Currently available AF recording and processing technologies are mainly restricted to specific applications or have technological limitations. Improvements in AF mapping by obtaining highest fidelity source signals (e.g. catheter–electrode combinations) for signal processing (e.g. filtering, digitization, and noise elimination) is of utmost importance. Novel acquisition instruments (multi-polar catheters combined with improved physical modelling and ML techniques) will enable enhanced and automated interpretation of EGM recordings in the near future.

Keywords   Atrial fibrillation • Signal recording • Signal processing • Mapping • Machine learning • Cardiac implantable electronic devices • EHRA position paper

Introduction

Recording, processing, and subsequently interpretation of electrical activity of the atria is essential for diagnosis and guiding (ablation) therapy of atrial fibrillation (AF). Atrial electrical activity in clinical practice can be measured using body surface electrocardiograms (ECG) or endo- and epicardial electrograms (EGM); optical action potentials are also used in research settings. The ECGs recorded by implantable loop recorders or EGMs by pacemaker and implantable cardioverter-defibrillators (ICDs) can be used for AF detection.

In the electrophysiology laboratory, analysis of EGMs recorded by catheters plays an important role in adjunctive ablation strategies performed in addition to pulmonary vein isolation, particularly in patients with (longstanding) persistent AF. However, electrical activity during AF is highly complex requiring advanced mapping systems equipped with sophisticated processing technologies for identification of suitable target sites for ablation. As standard approaches for recording and processing electrical activity during AF do not exist a lot of effort has been put in clinically evaluating a variety of mapping systems yet with mixed outcomes. Many of the currently available recording and processing technologies are also restricted to specific applications or have technological limitations hampering wide-spread applicability. Importantly, guidelines or recommendations in this area currently do not exist.
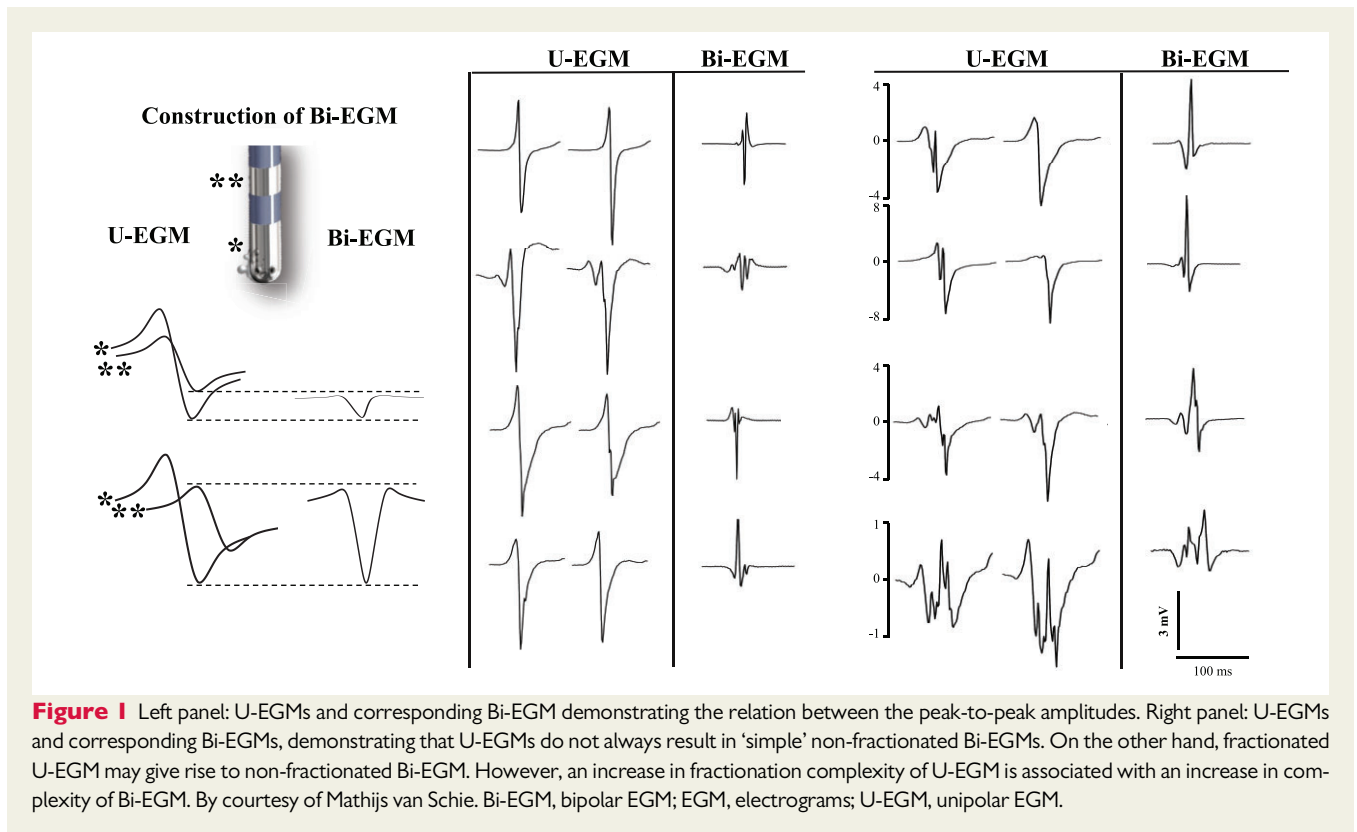
Aims and scope

The objectives of this document are to (i) provide a critical appraisal of basic concepts underlying signal recording and processing technologies applied for AF mapping to unravel AF mechanisms and/or identifying target sites for AF therapy and AF detection, (ii) discuss clinical values and limitations based on unique features of these technologies, (iii) advise on their applications, and (iv) to identify unmet needs in context of signal recording and processing. This position paper provides up-to-date knowledge for clinicians, engineers, and researchers to optimize usage of signal recording and processing methodologies, stimulate research aimed at closing knowledge gaps and developing ideal AF recording and processing technologies. As novel signal recording and processing technologies are continuously being developed, we do not aim to review all features offered by currently existing mapping systems.

Electrograms

Unipolar and bipolar electrograms

An EGM is the extracellular potential difference between two adjacent electrodes [bipolar (Bi-EGM)] or the potential difference between one single electrode in tissue contact relative to an indifferent electrode at zero potential or Wilson Central Terminal [unipolar (U-EGM)]. *Figure 1* shows examples of U-EGM and corresponding Bi-

Figure 1 Left panel: U-EGMs and corresponding Bi-EGM demonstrating the relation between the peak-to-peak amplitudes. Right panel: U-EGMs and corresponding Bi-EGMs, demonstrating that U-EGMs do not always result in 'simple' non-fractionated Bi-EGMs. On the other hand, fractionated U-EGM may give rise to non-fractionated Bi-EGM. However, an increase in fractionation complexity of U-EGM is associated with an increase in complexity of Bi-EGM. By courtesy of Mathijs van Schie. Bi-EGM, bipolar EGM; EGM, electrograms; U-EGM, unipolar EGM.

EGM recorded during AF.[1,2] Although AF mapping is most frequently performed with Bi-EGM, U-EGM are nowadays also increasingly being used. So far, differences between U-EGM and Bi-EGM for AF mapping have only been examined for identification of low-voltage areas in single centre clinical studies and experimental studies (Voltage mapping section) and of endo-epicardial asynchronously activated areas in experimental studies (Epicardial mapping of AF section). The advantage of U-EGMs is that determination of local activation time (LAT) is straightforward (LAT mapping section). The main disadvantage of U-EGMs is that local fibrillation potentials may be masked by far-field potentials or distant atrial activity caused by the ventricles and multiple fibrillation waves, as U-EGMs are sensitive to remote electrical activity. So far, in only one report, U-EGM features (dV/dT_{max}< 0.05 V/s, amplitudes < 0.2 mV, and durations > 35ms) used to discriminate local from far-field fibrillation potentials have been described.[3] The major advantage of Bi-EGM is its relative insensitivity to remote electrical activity and electrical noise (due to common mode rejection) and it is therefore often the preferred recording mode used for AF mapping.[1,2] However, a disadvantage of Bi-EGM is that its amplitude depends on wavefront direction; when a fibrillation wave passes both electrodes at the same time, subtraction of virtually equal U-EGMs results in no residual Bi-EGM. Annotation of LAT is also more ambiguous (LAT mapping section). In addition, Bi-EGM morphology not only depends on inter-electrode spacings,[4] but also on conduction velocity (CV) and direction of the fibrillation waves which both vary from beat-to-beat during AF.

Thus, Bi- and U-EGM have their own (dis) advantages (Table 1) for AF mapping and their morphology is affected by various variables

(see Supplementary material online, Table S1). At present, there are no clinical studies demonstrating that either U- or Bi-EGM are more suitable for AF mapping. As they provide complimentary information, combined usage for AF mapping could be beneficial.

Multi-polar electrograms

Multi-polar EGM include Laplacian and omnipolar EGMs (Figure 2). Laplacian EGMs are calculated by subtracting the centre electrode U-EGM from the U-EGM of either evenly distributed surrounding close-by electrodes, (fixed electrode-array), or sequentially obtained EGMs weighted for distance utilizing an electro-anatomical mapping system.[5] If electrodes are close together, Laplacian EGMs approximate the second-order spatial derivative of the U-EGM. Omnipolar EGMs yield EGMs independent from the orientation of the recording electrodes, and hence wavefront direction. They are calculated within a clique, which is defined as a square of four electrodes from which the Bi-EGM with the largest amplitude is extracted.

Experiences with multi-polar EGMs such as Laplacian and omnidirectional EGMs during AF are limited to voltage mapping in experimental settings in canine and human atria.[5,6] Table 1 summarizes (dis)advantages of omnipolar and Laplacian EGMs. So far, there are no clinical studies demonstrating advantages of multi-polar EGM over U- and Bi-EGM for AF mapping.

Impact of recording technology on electrograms morphology

The EGM morphology is affected by the size of recording electrodes, shapes of electrodes (printed on splines or integrated in catheter shaft), inter-electrode distances, filtering, and the sampling rate of

Table 1 Advantages and disadvantages of uni-, bi-, and multi-polar EGMs

EGM	Advantages	Disadvantages
Unipolar	• LAT: inambiguous, wavefront direction independent • Morphology: information on wavefront characteristics	• Sensitive to remote electrical activity
Bipolar	• Insensitive to remote electrical activity	• LAT: ambiguous • Morphology: depends on inter-electrode distances, CV, wavefront direction
Multi-polar	• Insensitive to remote electrical activity • LAT: less ambiguous, less wavefront direction dependent than bi-EGM • Amplitude: less wavefront direction dependency than bi-EGM	• Loss of spatial resolution • Additional computational efforts • Electrode distance should be ≤1 mm (Laplacian only) • Specialized dedicated electrode array, electro-anatomical mapping systems.

CV, conduction velocity; LAT, local activation time.
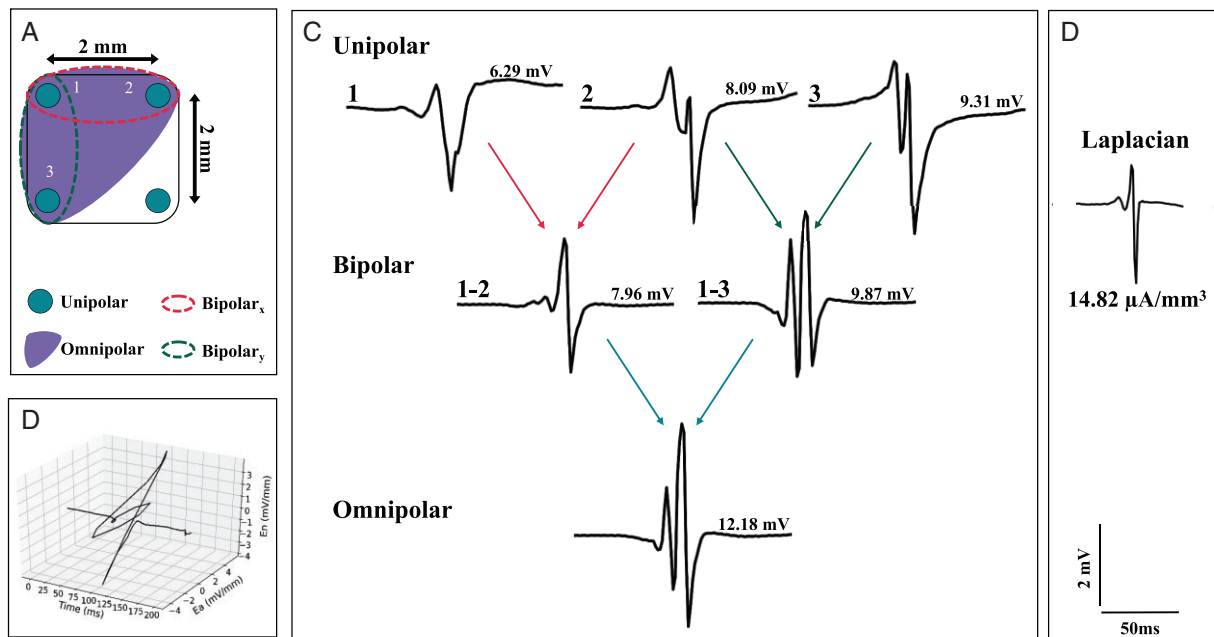
Figure 2 (*A*) Cliques enclosed by four electrodes are used to record three U-EGM (filter: 5–400 Hz) visualized in the top of (*C*). The U-EGMs of three adjacent electrodes (1,2, and 3) are used to derive Bi-EGM by subtracting one U-EGM from the other U-EGM such that two pairs of Bi-EGMs (1–2 and 2–3) are constructed along the horizontal (red) and vertical (green) directions. Bi-EGMs are filtered (30–400 Hz) and visualized in the centre of (*C*). Both Bi-EGMs are used to describe a depolarization wavefront as an electrical field which is electrode orientation-independent. (*B*) Illustrates the projections along the time-axis of the electrical field derived from both Bi-EGMs. This enables to mathematically obtain Bi-EGMs in any direction without physically rotating a sensing electrode. The E-field is subsequently scaled to analogous 2D voltage signals from which the maximal extent over the interval (*T*) is calculated and corresponds to the peak-to-peak amplitude of a Bi-EGM obtained along a unit vector direction. (*C*) Resulting omnipolar EGM, (*D*) corresponding Laplacian EGM. By courtesy of Mathijs van Schie. Bi-EGM, bipolar EGM; EGM, electrograms; U-EGM, unipolar EGM.

digitization (see Supplementary material online, *Table S1*). Smaller diameter electrodes result in higher frequency and amplitude potentials of both U- and Bi-EGM[7] but also higher noise levels caused by higher input impedances.[8,9] A decrease in inter-electrode distances is associated with a decrease in voltages and fractionation.[10,11] Filtering and the sampling frequency also influence EGM characteristics.[12] According to the Nyquist principle, the sampling rate should be at least twice the highest intended frequency content to be measured.

Filtering may attenuate respiration or movement artefacts, interference and far-field components, but it also affects EGM morphology.[1,2,9] Especially high-order filters that attenuate certain frequencies more steeply, may disturb EGM morphology significantly.[9,12] Such filters are prone to ringing and may generate artificial deflections. Low- and high-pass filtering may, respectively, increase and decrease amplitudes of U-EGM; both low- and high-pass filtering decreases fractionation of U-EGM recorded during AF.[1,9] Notch filtering increases fractionation of U-EGM during AF and reduces amplitudes.[9] Hence, filtering significantly affects the already complex morphology of EGM recorded during AF and should therefore be avoided as much as possible.

Invasive mapping of atrial fibrillation

Local vs. global mapping modes

Cardiac mapping is defined as a methodology by which electrical potentials recorded from the heart are spatially depicted in an integrated manner, usually as a function of time.[13] Identification of underlying mechanism(s) and arrhythmogenic substrates by mapping of AF is slowly progressing. In contrast to mapping uniform arrhythmias with a stable and defined focal or re-entrant mechanism, AF mapping is challenging, as AF is neither purely focal nor stable re-entry in nature.[14,15] Thus, conventional mapping catheters and algorithms assuming spatiotemporal EGM stability are not applicable to AF mapping. There is no consensus on how long AF episodes should be recorded to obtain a representative value of a specific parameter and how to determine the electropathological variable which most accurately represents arrhythmogenic tissue (e.g. mean, median, or ranges). Two concepts for recording of electrical activity during AF are 'global' and 'local mapping'.

Global atrial fibrillation mapping

Global mapping ('panoramic view') refers to simultaneous recording of EGMs of the entire atria using large intra-cardiac basket catheter(s) (see Supplementary material online, *Figure S1*) or body surface electrodes (Non-invasive mapping of AF section). Endocardial, multi-electrode basket catheters record up to 128 U-EGMs simultaneously from multiple locations and can be used for e.g. activation or phase mapping. Bi-atrial activity is recorded during a single interval which avoids interpolation associated with combining sequential data from multiple intervals.

Non-randomized clinical studies demonstrated that ablation targeted at stable rotational activity and focal sources could eliminate AF.[16,17] Algorithms using data recorded by these basket catheters are often biased towards detection of rotational activities even when these do not exist; focal activation might be displayed as rotational activity if the wavefront reaches surrounding electrodes sequentially.[18,19] Advantages of these catheters are that they measure contact EGMs and allow real-time evaluation of propagation for guiding ablation. However, they also have significant limitations: (i) suboptimal electrode–tissue contact at many poles; (ii) splines are not equidistantly separated, (iii) low spatial resolution, (iv) lack of reproducible positioning, (v) recordings contain spline touch artefact's, (vi)

higher pro-coagulative tendency, (vii) septum and coronary sinus are not included. Additionally, the amount of extrapolation used for construction of e.g. activation time maps is difficult to determine. Although initial, non-randomized studies in patients with AF were promising, a randomized, controlled, multi-centre clinical trial failed to demonstrated successful outcomes of ablative therapy guided by global mapping.[20]

Local atrial fibrillation mapping

Local mapping refers to high-density mapping of smaller regions using contact multi-polar catheters; the catheter moves consecutively through the atria to obtain local electrical activity.

During local mapping, contact catheters directly record, rather than estimate, EGMs. This can be achieved epicardially with high-density electrode grids placed during surgery[21] or endocardially with multi-electrode mapping catheters introduced percutaneously (see Supplementary material online, *Figure S1*).[22] The resulting maps have a high local resolution but however, limited global resolution. Maps created with roving catheters often utilize Bi-EGM rather than U-EGM. A benefit of multi-electrode mapping catheters over linear ablation catheters is the higher likelihood that electrodes are in contact with tissue, reducing the effect of catheter angle on EGM morphology.[23–25] Also, multi-electrode grids allow fixed uniform and reproducible interpolation unlike spline or basket multi-electrode catheters.

Multi-electrode mapping catheters with smaller electrodes and closer inter-electrode spacing increase the mapping resolution.[22,26] However, the optimal mapping resolution during AF is yet to be defined. Also, the larger number of data points recorded by multi-electrode mapping catheters precludes real-time manual annotation of individual signals, thus, creating dependency on automated algorithms and their accuracy. Simultaneous construction of endocardial and epicardial contact maps accounting for transmural activation sequences may be warranted in AF but has not yet been clinically implemented.[3]

Signal processing technologies

Signal processing refers to analysis, usually automated, of EGMs. Analysis is focused on identifying specific parameters defining individual EGM characteristics with the principal aim of rapidly interrogating the arrhythmogenic substrate and targeting sites critical to AF maintenance. Various signal processing techniques applicable for AF mapping discussed below are summarized in *Table 2*.

Local activation time mapping

A LAT map depicts the activation time at every recording site relative to a reference point.[27,28] The LAT mapping is used to visualize patterns of activation to e.g. discriminate between re-entry and focal activity or to identify slow, crucial zones of slow conduction by superimposing isochrones. *Figure 3* illustrates examples of difficulties encountered in annotation LAT of U- and Bi-EGM. The LAT maps using U-EGM are based on the principle that the timing of $-dV/dT_{max}$ coincides with the time of maximum rate of rise of the transmembrane potential (time differences less than $50\,\mu s$[29]) corresponding to the maximum increase in sodium current and its conductance. The

Table 2 Summary of signal processing technologies

Analytic technique	Rationale	Assumption	Principal issue(s)	Processing requirements	Real-time use	Evidence	Clinical status
LAT maps	Temporo-spatial sequencing	EGM reflects unique discrete myocardial depolarization	Sequencing ≠ mechanism; 3D simplified to 2D	AD conversion, data storage, Limited algorithmic processing	Nearly real-time	Extension of organized tachyarrhythmias; animal AF models	Data supporting clinical feasibility but not ablation
Voltage maps	Delineation of electrically inactive/less active areas based on EGM voltage	Reduced EGM voltages reflect desynchronization and fibrous tissue	Multiple possible confounders of EGM voltage	Minimal	Yes	Fibrosis, scarring in animal ventricular infarct models	Easily available, but not 'well established'
CFAE maps	Short interval multi-deflection or continuous EGM representing driver sources, re-entry	CFAEs represent multi-wavelet driver sources not passive fibrillatory conduction	Multiple definitions of CFAE; lack of convincing evidence of driver role	Minimal	Yes	Human AF epicardial mapping, some outcomes of CFAE-based ablation	Easily available but no standardized definition; also not 'well established'
Density charge maps	Improved resolved local activation compared with EGM voltage	Mathematical derivation of endocardial surface projected EGM from non-contact U-EGM and corrected for 'charge density' promising lesser far-field effects	Mathematical assumptions involving reconstructed EGM prominent effects of distance—accuracy and validation concerns—reminiscent of a legacy non-contact mapping technology	Substantial and proprietary	Sufficiently rapid to be usable in the EP lab	Limited correlations with contact mapping in AF and SR	Single beat 'panoramic' chamber mapping ability attractive but further validation of complex activation needed
Rotor maps	Phase 'reconstruction' without LAT determination allows detection of functional re-entry without central inexcitable obstacle as preferential drivers	Rotors—a type of functional re-entry—the main driver source(s) which are not detectable without phase reconstruction	Phase mapping a form of low pass smoothing of low resolution U-EGMs underlying algorithm favours rendition of rotational activation	Proprietary algorithm, opaque processing	Sufficiently rapid to be usable in the EP lab but with offsite processing	Experimental studies, typically with action potential-based optical mapping	Controversial outcomes of ablation; non-standardized interpretation of phase maps

Continued

Table 2	Continued						
Analytic technique	Rationale	Assumption	Principal issue(s)	Processing requirements	Real-time use	Evidence	Clinical status
Body surface maps	ECG inversion allows non-invasive EGM reconstruction	Mathematical model of the thorax conductivity; anatomy obtained from MRI or CT	Numerical instability, poor resolution/time domain fidelity, motion artefacts	Large and mostly proprietary	Sufficiently rapid to be usable in the EP lab but with offsite processing	Experimental and clinical evidence	Single beat EGM reconstruction of the entire heart at relatively low resolution; further validation needed
Machine learning/AI	EGM-based training (big) data used by machines with a learning algorithm to identify drivers	Input data sets contain (a) valid envisaged solutions	Optimal gold standard for training yet to be identified; decision making tree opaque	Large	Intended for use in the lab with offsite processing	Identifying drivers in AF computational models	Undetermined

AD, activation direction; AF, atrial fibrillation; AI, artificial intelligence; Bi-EGM, bipolar EGM; CFAE, complex fractionated atrial electrograms; EGM, electrograms; LAT, local activation time; U-EGM, unipolar EGM.

LAT determination using Bi-EGM is more complex; bipolar LAT maps are constructed by annotating the onset, peak or $-dV/dT_{max}$ of Bi-EGM. An accurate algorithm for LAT annotation utilizes the $-dV/dT_{max}$ of the first-order spatial derivative of the underlying U-EGM. This assumes that shape and velocity of the propagating wavefront remains constant, which is usually not the case during AF. Activation time mapping is an effective approach if EGMs consist of a single negative deflection but is challenging if EGMs are fractionated or contain continuous electrical activities. Several advanced signal processing technologies have been proposed to improve automated analysis of complex EGMs, including investigation of signal morphology, wavelet decomposition, deconvolution, and wavefront tracking, yet clinical benefits of these technologies have not yet been demonstrated.[28,30–33]

Voltage mapping

A voltage (V) map depicts the peak-to-peak amplitudes of EGMs at multiple sites (see Supplementary material online, Figure S1). However, both unipolar (UV) and bi-polar voltage (Bi-V) are influenced by numerous variables (see Supplementary material online, Table S1). The UVs are larger than Bi-V; only when the maximum V at one electrode nearly coincides with the minimum V at the other electrode, then the V of the negative deflection of Bi-EGM equals the peak-to-peak V of U-EGM (left panel, Figure 1). Another determinant of EGM-V is rate and hence cardiac rhythm.[34] There is a modest correlation between Bi-V measured during AF and sinus rhythm, which becomes weaker in patients with more persistent types of AF.[35] The Bi-V are higher during sinus rhythm compared with AF. During atrial extra stimuli with decreasing coupling intervals, Bi-V were more attenuated than UV.[34] Despite numerous variables affecting EGM-V, low endocardial Bi-V are regarded as surrogate markers of fibrotic tissue and low-voltage areas have therefore become targets for ablative therapy in patients with AF.[36] It is important, however, to emphasize that there is limited data correlating low-voltage areas to mechanisms initiating or perpetuating AF.[36] Several definitions of voltage thresholds related to 'scar tissue' have been introduced e.g. 0.5 mV (most often used, 5th percentile obtained during supraventricular tachycardia), 0.05 mV (noise level electro-anatomical mapping system), 0.2 mV for the posterior left atrial wall (5th percentile of V histograms of patients with paroxysmal AF) or <0.1 mV ('dense scar', patients with persistent AF).[37–39] However, none of these thresholds have been validated pathologically and outcomes of ablation targeting bipolar low-voltage areas—either during sinus rhythm or AF—show conflicting results.[40] Possible explanations for these discrepancies include mapping and/or ablation strategies and patient selection. Also, since voltage depends on size and distances of electrodes, voltage maps acquired with different catheters should not be compared.

Complex fractionated atrial electrograms mapping

Complex fractionated atrial electrograms (CFAE) maps depict the location of CFAEs (see Supplementary material online, Figure S1). The CFAE are most often defined as potentials with three or more negative deflections. However, in literature, at least 27 different definitions and/or methodologies for identification of CFAE have been
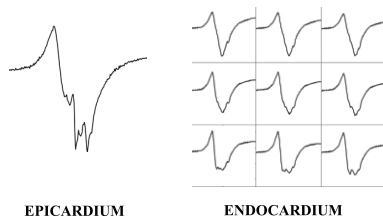
Annotation Uncertainties

A   LAT Estimation
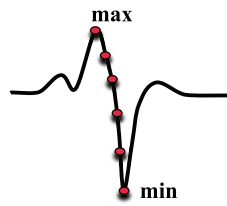
B   Fractionation
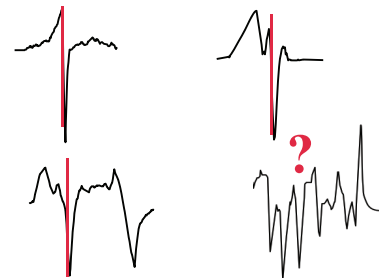
C   Endo-epicardial Asynchrony

D   Filter settings

Figure 3 Challenges encountered with annotation of potentials recorded during AF. (*A*) Red dots indicate the different time samples. Annotation of the steepest deflection can be calculated by e.g. averaging the steepest deflection of all time samples, selecting time samples with the steepest deflection, or averaging between maximum and minimum values. This information is usually not provided in manuals or in methodology sections of scientific reports. (*B*) In case of multiple deflection with comparable slopes and amplitudes, additional criteria have to be developed to determine local activation times (LAT). (*C*) As a result of endo-epicardial asynchrony, endocardial LATs may be different from epicardial LATs. (*D*) Determination of LAT is affected by the filter settings which has a considerable impact on U-EGM morphology. AF, atrial fibrillation; U-EGM, unipolar EGM.

Table 3   Complex fractionated electrograms

Variations in recording methodology	Variations in definition
• Bi-EGM	• Number of deflections
• U-EGM	• EGM duration
• Endocardial EGM	• Interval duration between deflections
• Epicardial EGM	• No. of short duration intervals between deflections
• Electrode sizes	• Amplitudes of deflections
• Inter-electrode spacings	• Slopes of deflections
• Filter settings	• Number of polarity changes of deflections
• Sampling rates	
• Rhythm/rate	

Bi-EGM, bipolar EGM; EGM, electrograms; U-EGM, unipolar EGM.

introduced (*Table 3*).[41] A review of 84 studies targeting CFAE, reported on absence of CFAE predilection sites in the right or left atrium and also no differences in degree of fractionation between patients with paroxysmal or persistent AF.[41,42] These findings are, however, not surprising, giving the variable methodologies applied. Also, how fractionated Bi-EGM should be correctly annotated is unknown. The mechanistic role of CFAEs in AF stems from the earlier work by Konings *et al.*[43] who performed unipolar epicardial mapping of induced AF in patients with Wolff–Parkinson–White syndrome undergoing cardiac surgery. By comparing U-EGM morphology and underlying activation patterns, they demonstrated that CFAEs during AF correlated to sites of pivot points and slow conduction. This led to the conclusion that CFAE areas during AF represent either continuous re-entry of fibrillation waves into the same area or overlap of different wavelets entering the same area at different times. This observation supports the hypothesis that AF is driven and maintained by multiple wavelets. Kalifa *et al.* proposed that fractionation occurs due to interruption of an activation wavefront as it crosses from one tissue boundary into another.[44] This hypothesis supported the observation that fractionation was highest at boundaries of dominant frequency (DF) domains (i.e. sites of highest DF and lowest frequencies) caused by differences in electrophysiological properties (refractory periods, CV, etc.) of adjacent myocardial tissue. These findings not only dispute the multiple wavelet hypotheses but also propose that (i) AF is driven and maintained by rotors and CFAE are located adjacent to sources, (ii) these sources correlate to sites of highest DF and highest regularity index (RI) i.e. sites of fastest and most organized activity, and (iii) that creation of borders at CFAE sites results in AF termination. However, others argued that there is only a modest spatial correlation between CFAE sites and highest DF and with the different responses to ablation at these sites,
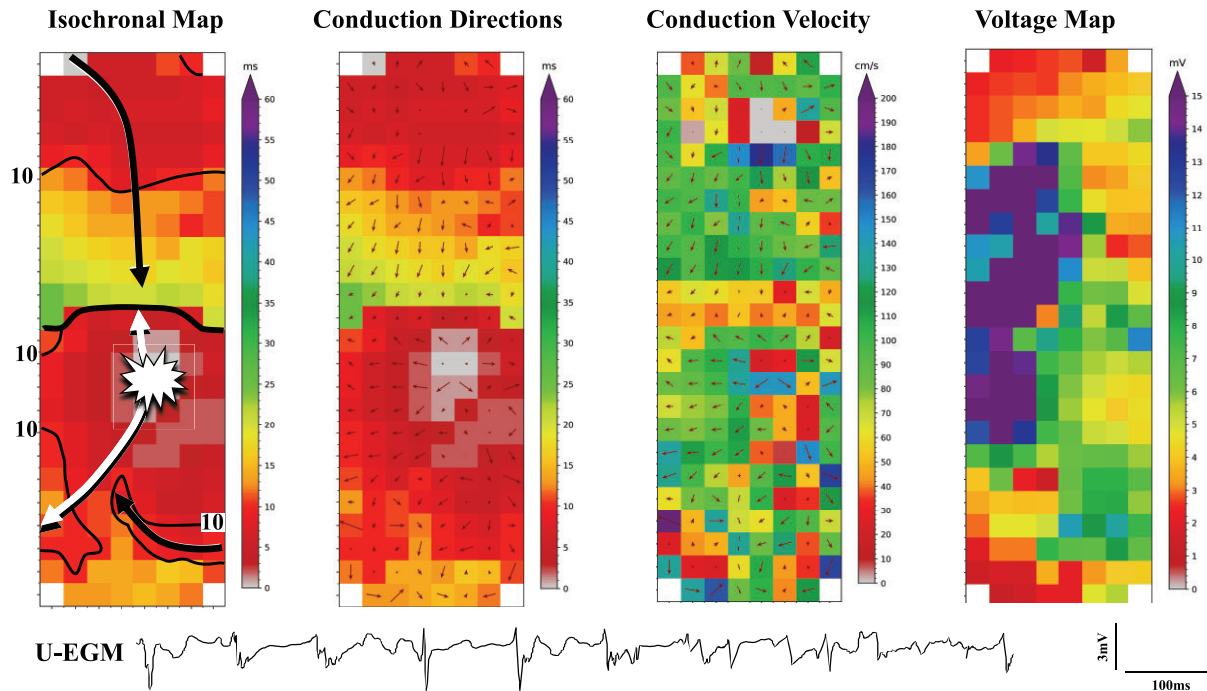
Figure 4 High resolution maps of the left atrial wall (*N*=192, inter-electrode distance 2 mm) constructed during AF obtained from a patient during cardiac surgery. These maps demonstrate from the left to the right: activation times combined with isochrones, local conduction directions, conduction directions and magnitude of conduction velocities, peak-to-peak voltages. By courtesy of Mathijs van Schie. AF, atrial fibrillation.

respectively, this may indicate that CFAE and DF domains are separate entities.[45] A multi-centre, randomized trial indeed demonstrated that CFAE ablation did not reduce AF recurrences on the long-term.[46,47]

Dipole density mapping

Dipole density mapping refers to utilization of dipole density—defined as 'cellular charge sources'—to resolve local electrical activation.[48,49] Data from an ultrasound array are used for reconstruction of the anatomy.[49] Non-contact electrodes sense intra-cavitary U-EGMs from which dipole densities are derived based on the precise ultrasound measured distance and reconstructed endocardial surface area. From these dipole densities, forward-calculated EGMs are reconstructed. A prediction model instead of data interpolation is used between the measuring points. Fundamental differences between voltage and dipole density lie in the averaging effect of 'spatial summation' and in the volume of space occupied by each. Theoretically, dipole density-based mapping provides a more localized portrayal of activation patterns than voltage-based mapping does, and with less far-field interference.

The accuracy of non-contact dipole density map was compared with contact voltage mapping during sinus rhythm and AF and correlated well when the recorded sites were ≤40 mm from the endocardial surface, comparable with previously published for non-contact mapping systems.[50] The theoretical benefits of dipole density mapping and initial clinical outcomes from single centre studies require further validation in randomized controlled trials.[50,51]

Rotational activity mapping

Rotational activity is caused by functional re-entry circuits (see Supplementary material online, *movie 1*) with an excitable but non-excited core and a curved wavefront subject to source-sink mismatch driving spiral waves.[52] Phase analysis is used to identify rotors based on identification of the phase singularity point and thereby the core of rotational activity driving AF. In phase mapping, the converted EGM is mathematically transformed to capture wavefront dynamics through the activation-recovery cycle of the underlying tissue, effectively functioning as a low-pass filter implemented on fractionated EGMs.[53] Phase analysis is particularly suited to optical mapping of action potentials with their characteristic depolarization upstroke, intervening plateau, and repolarization downslope and has been used effectively for AF analysis in experimental models.[54] However, as the type of signals recorded, and the technique employed influences phase analysis it remains unclear whether rotational activity seen during mapping of AF in humans is representative of the same re-entry mechanism demonstrated with optical mapping.[55] In computational and experimental models, rotational activities maintain AF and therefore have been considered ablation targets. Limitations of mapping in humans that may influence the phase analysis and thereby interpretation of phase maps includes: (i) artefact due to noise, (ii) far-field ventricular signals, and (iii) limited resolution with mapping catheters particularly basket catheters resulting in data interpolation. Interpolation of phases may result in representation of non-existent rotors as the interpolation algorithm is devised to detect rotational activity.[18,19,56]

Therefore, it remains unclear whether the current mapping modalities available in humans are able to effectively identify source mechanisms that have so elegantly been demonstrated in animal models with optical mapping. Furthermore, characteristics of these localized sources remain unclear. Spatiotemporal stability of rotational activities has been demonstrated in optical mapping studies in animal models, however, mapping of rotational activity in humans has shown inconsistent results.[16,17,57,58] While some studies conclude that these drivers are spatiotemporally stable[16] others have shown that even though spatially stable the drivers elicit temporal periodicity.[57] It remains unclear which of these characteristics are the correct description of these drivers and if both are, does the temporal stability have an impact on the mechanistic importance of these drivers? These questions remain to be answered.

Atrial rate analysis

The activation rate of a recording site can be estimated in the time domain in terms of average cycle length, while several indices related to activation organization can be obtained from the dispersion of the cycle length histogram. However, this approach requires the use of automatic algorithms to estimate LATs or cycle lengths, which can be challenging in case of CFAE.[59] Atrial rate can also be computed in the frequency domain, avoiding the need of LAT detection. In order to ensure that the maximum spectral amplitude corresponds to the atrial rate and not to one of its harmonics, Botteron's pre-processing[60,61] is applied to the raw signal before computing the spectrum. This pre-processing (see Supplementary material online, *Figure S2*) consists of three steps: band-pass filtering, rectification, and low-pass filter removing details of the individual activations and converting the raw signal in a train of smooth pulses. The DF is defined as the highest spectral peak of this pre-processed signal. The organization index has been defined as the ratio of the spectral power around the DF and its harmonics to the total spectral power.[62] This index measures the periodicity of the pre-processed signal, which is a sign of periodic and organized activations. Spatial distribution of activation rate and activation organization has been studied to find AF critical sources, and therefore, candidate sites for ablation, based on the hypothesis that high activation rates and organization allows identification of sources driving AF.[63] While reduction of DF has been shown to be a marker of good ablation outcome,[64] direct ablation of sites with maximum DF have shown mixed results.[65–67]

Conduction velocity and activation direction analysis

Conduction velocity (CV) along a given activation direction (AD) can be measured from differences of LATs at electrodes with known two-dimensional inter-electrode distances (*Figure 4*).[28,68,69] However, CV can only be estimated as the true three-dimensional pathway is unknown. The CV can be semi quantitively visualized by construction of isochronal maps. Model-based approaches have been used to estimate both CV and AD, using LAT from EGMs recorded by circular catheters or multi-electrode arrays.[68] In general, CV and AD maps can be obtained by post-processing activation maps if they have enough spatial resolution,[70] but they may be very sensitive to errors and inconsistencies in LAT estimates. To cope with this problem, Anter *et al.*[69] proposed a method which estimates

a consistent global pattern of activation in the whole chamber, taking into account all candidate LATs in a single EGM, and then locally estimated CV and AD. Uncertainties in LAT estimation have been quantified and used for LAT interpolation.[71] Recently, van Schie *et al.*[72] introduced a novel, modified discrete velocity vectors methodology to calculate CV. The CV during AF is calculated to identify areas with low CV associated with structural remodelling. However, as the true pathlength is unknown, particularly in complex patterns of activations during AF, the calculated 'effective' CV may only be roughly estimated.

Entropy

Entropy is a dimensionless parameter of randomness, used in information theory to measure information content, estimate signal variability, or randomness in time series data and can therefore be used to evaluate EGM complexity objectively.[73] When applied to EGMs, low values indicate high regularity and predictability whereas high values increase progressively with irregularity and are highest for random noise. The amplitude histogram-based Shannon entropy measure was only moderately inversely correlated with CFAE.[73] A recent single centre study demonstrated that sample entropy, which uses EGM segment vector comparisons, is correlated with outcomes of ablation therapy in persistent AF patients undergoing CFAE ablation.

Non-invasive mapping of atrial fibrillation

The ECG Imaging (ECGI) is a non-invasive, body surface mapping technique (*Figure 5*) for reconstruction of cardiac excitation patterns using 80–250 electrodes applied to the upper torso.[74–76] Prior to this, the cardiac anatomy and electrode positions are determined either via medical imaging (CT or MRI scans) or with 3D localization technology.[74,77] Numerical inversion provides real-time estimates of epi- and endocardial U-EGMs, excitation wavefronts, or transmembrane voltages. From these, atrial maps of various quantities (e.g. activation time, voltage, phase, CV, and DF) can be derived and specific phenomena can be localized (e.g. ectopic foci, phase singularities, and rotors/rotor densities). Because of severe numerical problems, only a few investigators attempted to estimate transmural potentials. Inversion requires an accurate forward model including a source and an observation model. The observation model is a volume conductor model of the torso relating cardiac sources to body surface potentials. Relatively large distances between sources and electrodes translate into spatial blurring which the inversion tries to correct, but this is complicated as there are far fewer electrodes than source locations. The source model describes generation and spatiotemporal propagation of excitation, and depends on many hidden parameters—this serves as a prior to the solution. In practice, this is replaced by patient-independent assumptions and constraints on spatiotemporal smoothness. Priors are needed for regularization, because inversion is inherently an ill-posed problem with ambiguous solutions. Current systems reach resolutions of 10–20 mm, with wide standard deviations.[78] Temporal fidelity is often limited; estimated activation times have errors of 10–20 ms. Also, artefacts like spurious lines of
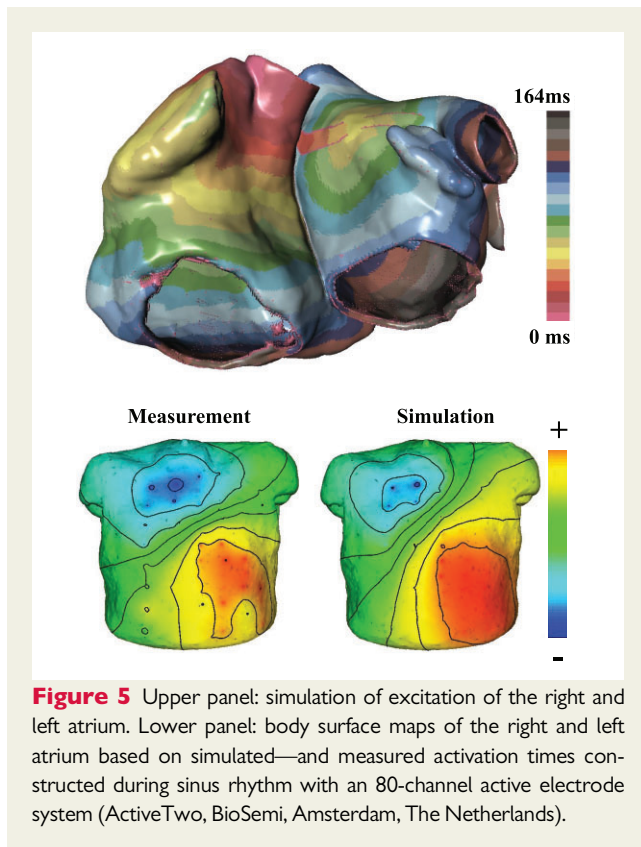
Figure 5 Upper panel: simulation of excitation of the right and left atrium. Lower panel: body surface maps of the right and left atrium based on simulated—and measured activation times constructed during sinus rhythm with an 80-channel active electrode system (ActiveTwo, BioSemi, Amsterdam, The Netherlands).

block are reported.[79] Due to their lower amplitude, atrial signals are harder to reconstruct than ventricular signals.

The promise of ECGI is that it will provide clinicians with non-invasive panoramic maps before the patient moves into the EP-lab, allowing anatomic characterization and localization of AF drivers, and therefore targets for ablation prior to procedures.[57] The ECGI could also help verify permanent post-ablation conduction block or identify gaps in ablation lines before re-do procedures.[80] As a research tool, ECGI provides a means of studying AF and poorly understood mechanisms like re-entry circuits, rotors, and rotor densities, areas of slow conduction, focal sources, CFAEs, and DF heterogeneities.[81] Combined with LGE-MRI, it can identify locations where rotors anchor to fibrotic substrates—potential ablation targets.[82]

However, validation of ECGI remains a significant challenge. Comparison of ECGI with EGMs using an intra-cardiac catheter mapping showed general agreement with several important limitations,[53,83,84] primarily related to numerical challenges in the inversion. The technique is sensitive to ECG noise and motion (cardiac cycle, breathing), sometimes resulting in artefacts or outliers. Regularization techniques make generic assumptions on source parameters and it is unclear how that impacts accuracy. Detection of small amplitude EGMs or drivers with short cycle lengths using ECGI may not be reliable, in particular the assessment of drivers in the septal area is challenging. Moreover, the clinical workflow is complex, requiring application of an electrode vest, its anatomical registration and subsequent image processing that has not yet been fully

automated and may be hampered by patient-specific factors. This has limited its clinical adoption. Hence, translation of ECGI maps into reliable disease markers requires additional studies.[85]

Research tools for atrial fibrillation mapping

Optical mapping of atrial fibrillation

Optical mapping involves use of voltage-sensitive dyes to examine spatiotemporal excitation patterns in cardiac tissue (*Figure 6*).[86] This technique has been used in animal models to elucidate tissue-scale or organ-scale atrial electrophysiology, including characterization of anti-arrhythmic drug effects, understanding cellular and molecular AF mechanisms, and exploring the prospect of light-based optogenetic cardioversion.[86–88] In contrast to isolated cell models, optical mapping enables analysis of non-disrupted myocardium in its native electrophysiological milieu. Recent advances have evaluated interplays between three-dimensional tissue fibrosis and AF mechanisms.[89] These data have been used to calibrate computational models that realistically reproduced re-entrant arrhythmia drivers seen *in vitro*. Insights obtained from such studies may be useful to improve calibration of image-based computational models in contemporary studies.[90,91] Disadvantages of optical mapping include applicability to only *ex vivo* cardiac tissue construction of solely two-dimensional images. As a research tool, modern mapping technologies may integrate essential findings from optical mapping data specifically on large-scale tissue activation. Progress in this area will likely be hastened by the recent publication of open experimental protocols for relatively inexpensive construction of panoramic optical mapping systems.[92,93] Notably, interpretation of data from optical mapping could account for limitations of experimental systems, such as the absence of extracardiac sympathetic or parasympathetic regulation of Langendorff-perfused hearts. Moreover, recent findings show that usage of Blebbistatin to reduce motion artefacts in optically mapped hearts via blocking excitation–contraction leads to non-physiological action potential duration prolongation.[94]

Epicardial mapping of atrial fibrillation

Cardiac surgery offers the opportunity to perform mapping (*Figure 4*) of the atrial epicardium. Epicardial mapping can be performed with arrays containing a high number of electrodes (>100) with small diameters (0.4–0.6 mm) and inter-electrode distances (2–2.5 mm).[21,95] As these arrays are manually positioned on the epicardium, stable contact between electrodes and atrial tissue is ensured. Also, exact locations of the electrode array in relation to anatomical structures are visualized. Another advantage of this mapping approach is access to regions which cannot be reached from the endocardium such as Bachmann's Bundle.[96] Electrode arrays used during cardiac surgery records EGM at multiple sites simultaneously, which is essential for understanding AF mechanisms. Simultaneous mapping of the endo-epicardium during surgery has indeed unravelled endo-epicardial electrical asynchrony as potential novel mechanism underlying AF persistence.[3] A disadvantage is the sequential mapping approach and the electrode arrays are custom-made and therefore not clinical available. At present, there are no clinical studies
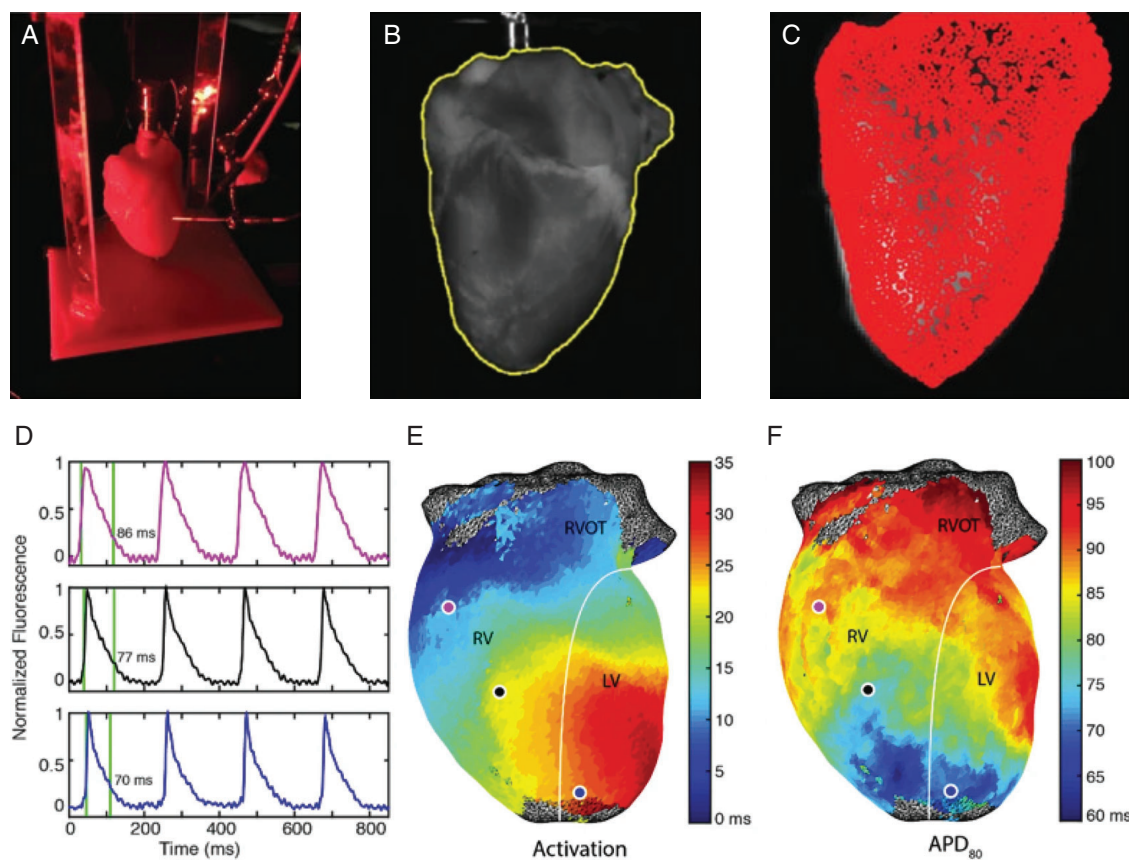
Figure 6 Schematic illustration of the use of an open source imaging toolkit for panoramic optical mapping, as described by Gloschat *et al.* (*A*) Experimental optical mapping setup, including Langendorff-perfused heart. (*B*) Heart image with superimposed silhouette (yellow) derived via an automated thresholding process. (*C*) Data projection points for reconstruction of panoramic maps of optically mapped data. (*D*) Examples of optically mapped action potentials recorded from the epicardial surface of a rat heart, including annotations for activation and 80% repolarization times. (*E* and *F*) Spatial reconstructions of activation time (*E*) and 80% action potential duration (*F*) from representative rat panoramic optical data. Images reproduced from *Figure 1 (A–C)* and Figure 7 (*D–F*) of Gloschat *et al.* under the terms of the Creative Commons Attribution 4.0 International License. To view a copy of this license, visit http://creativecommons.org/licenses/by/4.0/. [93]

demonstrating the value of epicardial mapping guiding (surgical) ablation procedures.

Detection of atrial fibrillation

Implantable cardioverter-defibrillator/pacemakers

In recent years, an increasing number of cardiac implantable electronic devices (CIEDs) have been implanted in patients with cardiovascular diseases. The CIEDs enable AF detection with storage of intra-cardiac EGM for evaluation at any time. As a result of continuous monitoring of a growing number of patients, AF detection has increased dramatically, potentially impacting therapeutic strategies.[97] Atrial high rate EGM (AHREs) are commonly used to detect AF. The AF detection algorithms vary between different CIEDs. Generally, in all CIEDs, the PP intervals are continuously monitored. Different models of associating the detected PP intervals to the programmed PP values are used to identify AF (*Table 4*). Moreover, it should be

noted that AF detection by CIEDs is not always correct, particularly when repetitive non-re-entrant ventriculo-atrial synchrony ensues.[98]

Implantable loop recorders

Implantable loop recorders (ILRs) with dedicated AF algorithms are used for diagnosis and monitoring of AF after surgical or catheter AF ablation, and cryptogenic stroke.[99–104] The ILRs have high accuracy in detecting AF burdens using incoherence of R–R intervals over a period of time.[105–108] Lorenz plots have extensively been used to demonstrate RR interval irregularity during AF and to discriminate between AF and sinus rhythm. Different ILR models equipped with algorithms for AF detection can accurately quantify AF burden (98.5%) and are very sensitive (96.4%) to identify asymptomatic patients with AF.[106,107] In order to reduce the rate of false positive AF episodes, an ILR with a long sensing vector has been utilized.[109] Moreover, ILR algorithms were improved to detect visible P waves in the absence of noisy baseline or flutter waves and were enhanced with artificial intelligence (AI) tools that learn if a patient has P-waves during periods of RR irregularity. Performance of AF detection

Table 4 Summary of the different AF detection algorithms

Type of CIED	Sensed signal	Methodology of AF detection
Dual chamber Pacemaker/ICD	Atrial EGM	The current PP interval of each beat is measured and the filtered atrial rate interval (FARI) is calculated. When FARI is less than the atrial tachycardia detection rate interval, AF is detected and the auto mode switch starts. This algorithm often overdiagnoses AF due to RNRVAS, particularly when the AF suppression algorithm is ON. In the most recent version of these pacemakers, P waves falling in the post-ventricular atrial refractory period are not taken into account in the FARI calculation when they are followed by atrial pacing, which prevents detecting RNRVAS as AF.
	Atrial EGM	AF is detected when the PP intervals in 3–8 out of 8 consecutive atrial cycles are less than the programmed PP interval. In the case of atrial tachycardia with 2:1 AV conduction, P waves often fall within the window of far-field protection, in which P waves are not taken into account for the atrial event rate, and atrial tachycardia is not detected (2:1 Lock-In). When specific criteria are met the atrioventricular delay is increased by the programmed far-field protection interval. If the P wave does not move with the ventricular paced events, atrial tachycardia is confirmed. Then, the pacemaker switches to a non-atrial tracking mode.
	Atrial EGM	PP intervals are continuously monitored. If a PP interval is faster than the ATR (Atrial Tachy Response) rate, the Entry Counter is incremented by 1 for each P wave. If a PP interval is slower than the ATR rate, the Entry Counter is decremented by 1. Once the counter reaches the programmed entry count (1–8), the duration starts.
	Atrial EGM	AF is detected when 4 out of 7 consecutive atrial intervals are shorter than the programmed AT/AF intervals.
	Atrial EGM	One or both the following conditions are needed for AF detection: (i) the median of 12 consecutive atrial intervals is shorter than the programmed AT/AF interval, (ii) the AT/AF counter is $\geq$3; the AT/AF counter is incremented by 1 point, each time $\geq$2 atrial events are sensed between one RR interval.
	Atrial EGM	The window of the atrial rate acceleration detection (WARAD) is used for the assessment of atrial prematurity. The WARAD is defined as the PP interval $\times$ 0.625 (if the atrial rate is $\geq$80/min) or 0.75 (if the atrial rate is <80/min). The primary criterion for the AF detection is the detection of a P wave within the WARAD in 28 out of 32 consecutive ventricular cycles. The secondary criterion is the P wave detection within the WARAD in $\geq$18 cycles of the last 2 sets of 32 consecutive ventricular cycles.
Single chamber ICD ILR	Ventricular EGM	Irregularity of RR intervals in Lorenz Plots.
	P wave and R wave	Irregularity of RR intervals, sudden onset, and absence of P waves.
	R wave	Irregularity of RR intervals and ectopy rejection algorithm.
	P wave and R wave	Irregularity of RR intervals, absence of P waves and AF self-learning algorithm.

All ILR algorithms showed a sensitivity and specificity ranging from 96% to 100% and 67% to 86%, respectively, for detection of AF episodes.
AF, atrial fibrillation; AT, atrial tachycardia; EGM, electrogram; ICD, implantable cardioverter-defibrillator; ILR, implantable loop recorder; RNRVAS, repetitive non-re-entrant ventriculo-atrial synchrony.

algorithms in ILRs depends significantly on the patient population, incidence rate of AF, duration of monitoring, and type of AF. For example, diagnostic sensitivity will get closer to 100% for longer monitoring duration or in patients with persistent AF.[108,110,111] Therefore, prolonged monitoring periods (> 3 years) are a prerequisite for the improvement of the ILR's diagnostic yield.

Post-processing of electrical signals

Advances in the field of Artificial Intelligence and in particular Machine Learning (ML), offer new opportunities to improve analysis of electrical signals.[112,113] Rapid progression in computational power, data storage, and remote data acquisition have enabled the application of ML to ECGs and EGMs.[112] Table 5 provides a non-exhaustive list of potential applications of ML in AF.[113,114] For the discussion of the application of AI for detection of AF we refer to recent scientific documents.[115,116]

The ML has several limitations and challenges. First, external validity and generalizability remain to be determined. The real value of this new approach in addition to clinical risk factors and risk scores requires further investigation and validation. Second, while large amounts of data can increase effectiveness of ML models, it is more difficult to critically assess their quality. Third, black box ML methodologies inhibit interpretation and make it impossible to involve

Table 5 AF and potential applications of ML

Holter long term/ CIEDs	• Determining AF burden
12-lead ECG	• P-wave detection and delineation • Dominant frequency determination • Finding episodes of AF • Identification of patients with AF while measuring during sinus rhythm
Body surface potential map	• Identification and localization, ectopic beats, rotors, and regions of high dominant frequency • ML-enhanced solutions of the inverse problem (ECGi)
Single or multi-channel EGM	• Estimation of proximity of electrodes to endocardial wall • Identification and delineation of time windows with high activity • Identification and localization of regions of low voltage or slow conduction • Identification and localization of lines of block • Estimating the vulnerability of the atria to develop AF in future • Identification of far-fields
LE-Gd-MRI	• Identification of areas with high fibrosis with ML-enhanced image processing • Estimate the risk of clinical events
General objectives with as many input channels as possible	• Quantification of the degree of disease for AF • Prediction of disease progression • Prediction of ablation outcome • Recommendation of the optimal ablation strategy

AF, atrial fibrillation; CIED, cardiac implantable electronic device; ECG, electro-cardiograms; EGM, electrograms; ML, machine learning.

stakeholders in meaningful shared decisions. Fourth, as we move away from intuition and physiologically reasoned model-based approaches towards large (and deep) multi-variate ML models, we lose interpretability and potentially increase the likelihood of catastrophic outputs, resulting in non-causal associations.

Conclusion

Recording and processing of EGMs are the cornerstones of mapping of AF. Yet, at present, it is unknown what the most ideal EGM recording type (e.g. uni-, bi-, or omnipolar) is and thus which technology should be used for recording and processing. The combination of a lack of golden standard of EGM recording and processing

technology during AF and of a comprehensive understanding of mechanism(s) underlying AF, does not give significant confidence in comparative evaluation of current technologies. The AI has opened a new era for signal processing, yet the clinical value still has to be further explored. The CIEDS are increasingly used to detect AF episodes, yet diagnostic yields need further improvement.

Suggestions according to the EHRA consensus documents classifications are summarized in *Table 6*.

Future perspectives

Improvements in AF mapping by obtaining highest fidelity source signals—including catheter–electrode combinations, to signal processing including filtering, digitization, and noise elimination is of utmost importance. The cleanest source signal, with minimal and/or clearly understood processing and a well-defined protocol facilitates evaluation and clinical application. A critical evaluation of signal recording and processing techniques takes into account all assumptions and mathematical transformations. Rigorous evaluation and validation of novel technologies involves e.g. large animal arrhythmia models and organized tachyarrhythmias before extending application to AF. Algorithms integrated in signal processing software should be provided in manuals and provided as supplements in scientific publications. Simultaneous multi-electrode activation time mapping, optimized for signal quality, electrode size, density, spacing, and coverage resolved to continuous high-fidelity propagation sequences with extraction of the arrhythmogenic substrate by automated software in near real-time enables minimally manipulated extraction of electrophysiological mechanisms underlying AF.

The ideal mapping system for AF should be able to automatically (i) detect noise sources and have an optimized noise removal thereby improving the signal-to-noise ratio, (ii) remove far-field QRS signal from the atrial EGM, (iii) annotate fibrillation potentials, and (iv) identify specific EGM features related to arrhythmia development or maintenance. The arrhythmogenic substrate underlying AF can be detected by AI and there is an integration of multi-parametric generated maps and images (e.g. MRI) with algorithms identifying sites of driver activity or specific substrate parameters related to AF and a validated support for identification of ablation targets. Finally, there is a real-time EGM monitoring to detect variations in AF maintaining mechanisms and display of multi-parametric maps.

The AF diagnostic yield of pacemaker/ICDs may be improved by enhancement of existing algorithms by use of RR interval irregularity detection algorithms. Furthermore, adequate atrial lead selection and positioning and optimal programming of atrial sensitivity may eliminate the effects of near-field P-wave or far-field R-wave oversensing by the atrial lead, runs of pre-mature atrial complexes, electrical interference, myopotentials, or repetitive non-re-entrant ventriculo-atrial synchrony on accurate AF detection.

For ILRs, further improvement in the AF detection algorithm should integrate rejection of ventricular extrasystoles in order to enhance the accuracy of AF diagnosis in patients presenting significant RR interval irregularities. Developments in multi-modal ML could be used for prediction and prognosis from multi-modal data (e.g. ECG, EGM, and LGE-MRI), improving understanding of the AF substrate, differentiating between paroxysmal AF and persistent AF, and

Table 6 Assessment of electrical activity during atrial fibrillation

- Combined usage of U-EGM and Bi-EGM For AF mapping, is advisable as they provide complementary information.
- Experience with multi-polar EGM for AF mapping is limited and their clinical advantages over U-EGM and Bi-EGM need to be elucidated.
- Filtering should be minimally applied during AF mapping.
- Global mapping requires extensive data interpolation and maps should be interpreted cautiously.
- Methodology of LAT determination should be described in detail in scientific reports.
- Voltage maps are influenced by many variables and are therefore less suitable to identify the substrate underlying AF.
- Although CFAE can be used as targets for ablative therapy, currently existing definitions of CFAE and recording methodologies have not been standardized and they are therefore at present not suitable to identify the substrate underlying AF.
- The value of artificial intelligence-guided substrate identification, dipole density maps, entropy graphs rotational activity, high atrial rates, areas of slow conductions as tools, or targets for substrate guided AF ablation procedures needs to be further elucidated.
- Optical mapping (applicable to *ex vivo* human hearts and large animal models only) and epicardial mapping are valuable tools for investigating AF mechanisms.
- AF detection algorithms in CIEDs can be further improved by combining RR-irregularities with Pwave features during long-term monitoring

Green heart: scientific evidence that treatment or procedure is beneficial and effective. Requires at least one randomized trial or is supported by strong observational evidence and authors' consensus.
Yellow heart: general agreement and/or scientific evidence favour usefulness/efficacy of treatment or procedure. May be supported by randomized trials based on small number of patients are not widely applicable.
AF, atrial fibrillation; Bi-EGM, bipolar EGM; CIED, cardiac implantable electronic device; CFAE, complex fractionated atrial electrograms; EGM, electrograms; LAT, local activation time; U-EGM, unipolar EGM.

predicting the outcome of ablation therapies. Recent developments in Generative Adversarial Network provide the potential to develop personalized models. Also, initial experiences with ML guiding substrate-based ablation therapy of AF have been published.[117–123]

Supplementary material

Supplementary material is available at *Europace* online.

References

1. Venkatachalam KL, Herbrandson JE, Asirvatham SJ. Signals and signal processing for the electrophysiologist: part II: signal processing and artifact. *Circ Arrhythm Electrophysiol* 2011;**4**:974–81.
2. Venkatachalam KL, Herbrandson JE, Asirvatham SJ. Signals and signal processing for the electrophysiologist: part I: electrogram acquisition. *Circ Arrhythm Electrophysiol* 2011;**4**:965–73.
3. de Groot N, van der Does L, Yaksh A, Lanters E, Teuwen C, Knops P *et al.* Direct proof of endo-epicardial asynchrony of the atrial wall during atrial fibrillation in humans. *Circ Arrhythm Electrophysiol* 2016;**9**:e003648.
4. Correa de Sa DD, Thompson N, Stinnett-Donnelly J, Znojkiewicz P, Habel N, Muller JG *et al.* Electrogram fractionation: the relationship between spatiotemporal variation of tissue excitation and electrode spatial resolution. *Circ Arrhythm Electrophysiol* 2011;**4**:909–16.
5. Coronel R, Wilms-Schopman FJ, de Groot JR, Janse MJ, van Capelle FJ, de Bakker JM. Laplacian electrograms and the interpretation of complex ventricular activation patterns during ventricular fibrillation. *J Cardiovasc Electrophysiol* 2000;**11**:1119–28.
6. Haldar SK, Magtibay K, Porta-Sanchez A, Masse S, Mitsakakis N, Lai PFH *et al.* Resolving bipolar electrogram voltages during atrial fibrillation using omnipolar mapping. *Circ Arrhythm Electrophysiol* 2017;**10**:e005018.
7. Beheshti M, Magtibay K, Masse S, Porta-Sanchez A, Haldar S, Bhaskaran A *et al.* Determinants of atrial bipolar voltage: inter electrode distance and wavefront angle. *Comput Biol Med* 2018;**102**:449–57.
8. Rocha PR, Schlett P, Kintzel U, Mailander V, Vandamme LK, Zeck G *et al.* Electrochemical noise and impedance of Au electrode/electrolyte interfaces enabling extracellular detection of glioma cell populations. *Sci Rep* 2016;**6**:34843.
9. Starreveld R, Knops P, Roos-Serote M, Kik C, Bogers A, Brundel B *et al.* The impact of filter settings on morphology of unipolar fibrillation potentials. *J Cardiovasc Transl Res* 2020;**13**:953–64.
10. Stinnett-Donnelly JM, Thompson N, Habel N, Petrov-Kondratov V, Correa de Sa DD, Bates JH *et al.* Effects of electrode size and spacing on the resolution of intracardiac electrograms. *Coron Artery Dis* 2012;**23**:126–32.
11. Takigawa M, Relan J, Martin R, Kim S, Kitamura T, Cheniti G *et al.* Detailed analysis of the relation between bipolar electrode spacing and far- and near-field electrograms. *JACC Clin Electrophysiol* 2019;**5**:66–77.
12. Stevenson WG, Soejima K. Recording techniques for clinical electrophysiology. *J Cardiovasc Electrophysiol* 2005;**16**:1017–22.
13. Yaksh A, Kik C, Knops P, Roos-Hesselink JW, Bogers AJJC, Zijlstra F *et al.* Atrial fibrillation: to map or not to map? *Neth Heart J* 2014;**22**:259–66.
14. Moe GK, Abildskov JA. Atrial fibrillation as a self-sustaining arrhythmia independent of focal discharge. *Am Heart J* 1959;**58**:59–70.
15. Moe GK, Rheinboldt WC, Abildskov JA. A computer model of atrial fibrillation. *Am Heart J* 1964;**67**:200–20.
16. Narayan SM, Baykaner T, Clopton P, Schricker A, Lalani GG, Krummen DE *et al.* Ablation of rotor and focal sources reduces late recurrence of atrial fibrillation compared with trigger ablation alone: extended follow-up of the CONFIRM trial (Conventional Ablation for Atrial Fibrillation With or Without Focal Impulse and Rotor Modulation). *J Am Coll Cardiol* 2014;**63**:1761–8.
17. Narayan SM, Krummen DE, Shivkumar K, Clopton P, Rappel WJ, Miller JM. Treatment of atrial fibrillation by the ablation of localized sources: CONFIRM (Conventional Ablation for Atrial Fibrillation With or Without Focal Impulse and Rotor Modulation) trial. *J Am Coll Cardiol* 2012;**60**:628–36.
18. Allessie M, de Groot N. Rebuttal from Maurits Allessie and Natasja de Groot. *J Physiol* 2014;**592**:3173.
19. Pathik B, Kalman JM, Walters T, Kuklik P, Zhao J, Madry A *et al.* Absence of rotational activity detected using 2-dimensional phase mapping in the corresponding 3-dimensional phase maps in human persistent atrial fibrillation. *Heart Rhythm* 2018;**15**:182–92.
20. Buch E, Share M, Tung R, Benharash P, Sharma P, Koneru J *et al.* Long-term clinical outcomes of focal impulse and rotor modulation for treatment of atrial fibrillation: a multicenter experience. *Heart Rhythm* 2016;**13**:636–41.
21. de Groot NM, Houben RP, Smeets JL, Boersma E, Schotten U, Schalij MJ *et al.* Electropathological substrate of longstanding persistent atrial fibrillation in patients with structural heart disease: epicardial breakthrough. *Circulation* 2010;**122**:1674–82.
22. Anter E, Tschabrunn CM, Contreras-Valdes FM, Li J, Josephson ME. Pulmonary vein isolation using the Rhythmia mapping system: verification of intracardiac signals using the Orion mini-basket catheter. *Heart Rhythm* 2015;**12**:1927–34.

23. Sroubek J, Rottmann M, Barkagan M, Leshem E, Shapira-Daniels A, Brem E *et al.* A novel octaray multielectrode catheter for high-resolution atrial mapping: electrogram characterization and utility for mapping ablation gaps. *J Cardiovasc Electrophysiol* 2019;**30**:749–57.

24. Huemer M, Qaiyumi D, Attanasio P, Parwani A, Pieske B, Blaschke F *et al.* Does the extent of left atrial arrhythmogenic substrate depend on the electroanatomical mapping technique: impact of pulmonary vein mapping catheter vs. ablation catheter. *Europace* 2017;**19**:1293–301.

25. Takigawa M, Relan J, Martin R, Kim S, Kitamura T, Frontera A *et al.* Effect of bipolar electrode orientation on local electrogram properties. *Heart Rhythm* 2018;**15**:1853–61.

26. Anter E, Tschabrunn CM, Josephson ME. High-resolution mapping of scar-related atrial arrhythmias using smaller electrodes with closer interelectrode spacing. *Circ Arrhythm Electrophysiol* 2015;**8**:537–45.

27. Ellis WS, Eisenberg SJ, Auslander DM, Dae MW, Zakhor A, Lesh MD. Deconvolution: a novel signal processing approach for determining activation time from fractionated electrograms and detecting infarcted tissue. *Circulation* 1996;**94**:2633–40.

28. Cantwell CD, Roney CH, Ng FS, Siggers JH, Sherwin SJ, Peters NS. Techniques for automated local activation time annotation and conduction velocity estimation in cardiac mapping. *Comput Biol Med* 2015;**65**:229–42.

29. Spach MS, Dolber PC. Relating extracellular potentials and their derivatives to anisotropic propagation at a microscopic level in human cardiac muscle. Evidence for electrical uncoupling of side-to-side fiber connections with increasing age. *Circ Res* 1986;**58**:356–71.

30. Bollacker KD, Simpson EV, Hillsley RE, Blanchard SM, Gerstle RJ, Walcott GP *et al.* An automated technique for identification and analysis of activation fronts in a two-dimensional electrogram array. *Comput Biomed Res* 1994;**27**:229–44.

31. Alcaine A, Soto-Iglesias D, Calvo M, Guiu E, Andreu D, Fernandez-Armenta J *et al.* A wavelet-based electrogram onset delineator for automatic ventricular activation mapping. *IEEE Trans Biomed Eng* 2014;**61**:2830–9.

32. Vidmar D, Alhusseini MI, Narayan SM, Rappel WJ. Characterizing electrogram signal fidelity and the effects of signal contamination on mapping human persistent atrial fibrillation. *Front Physiol* 2018;**9**:1232.

33. Ye Z, van Schie MS, de Groot NMS. Signal fingerprinting as a novel diagnostic tool to identify conduction inhomogeneity. *Front Physiol* 2021;**12**:652128.

34. Williams SE, Linton N, O'Neill L, Harrison J, Whitaker J, Mukherjee R *et al.* The effect of activation rate on left atrial bipolar voltage in patients with paroxysmal atrial fibrillation. *J Cardiovasc Electrophysiol* 2017;**28**:1028–36.

35. Ndrepepa G, Schneider MA, Karch MR, Weber S, Schreieck J, Zrenner B *et al.* Impact of atrial fibrillation on the voltage of bipolar signals acquired from the left and right atria. *Pacing Clin Electrophysiol* 2003;**26**:862–9.

36. Anter E, Josephson ME. Bipolar voltage amplitude: what does it really mean? *Heart Rhythm* 2016;**13**:326–7.

37. Sim I, Bishop M, O'Neill M, Williams SE. Left atrial voltage mapping: defining and targeting the atrial fibrillation substrate. *J Interv Card Electrophysiol* 2019;**56**:213–27.

38. Masuda M, Fujita M, Iida O, Okamoto S, Ishihara T, Nanto K *et al.* Left atrial low-voltage areas predict atrial fibrillation recurrence after catheter ablation in patients with paroxysmal atrial fibrillation. *Int J Cardiol* 2018;**257**:97–101.

39. Rodriguez-Manero M, Valderrabano M, Baluja A, Kreidieh O, Martinez-Sande JL, Garcia-Seara J *et al.* Validating left atrial low voltage areas during atrial fibrillation and atrial flutter using multielectrode automated electroanatomic mapping. *JACC Clin Electrophysiol* 2018;**4**:1541–52.

40. Spragg DD, Zghaib T. Veracity of voltage mapping during atrial fibrillation and flutter: how good is good enough? *JACC Clin Electrophysiol* 2018;**4**:1553–5.

41. van der Does LJ, de Groot NM. Inhomogeneity and complexity in defining fractionated electrograms. *Heart Rhythm* 2017;**14**:616–24.

42. Starreveld R, van der Does L, de Groot NMS. Anatomical hotspots of fractionated electrograms in the left and right atrium: do they exist? *Europace* 2019;**21**:60–72.

43. Konings KT, Kirchhof CJ, Smeets JR, Wellens HJ, Penn OC, Allessie MA. High-density mapping of electrically induced atrial fibrillation in humans. *Circulation* 1994;**89**:1665–80.

44. Kalifa J, Tanaka K, Zaitsev AV, Warren M, Vaidyanathan R, Auerbach D *et al.* Mechanisms of wave fractionation at boundaries of high-frequency excitation in the posterior left atrium of the isolated sheep heart during atrial fibrillation. *Circulation* 2006;**113**:626–33.

45. Kumagai K, Sakamoto T, Nakamura K, Nishiuchi S, Hayano M, Hayashi T *et al.* Combined dominant frequency and complex fractionated atrial electrogram ablation after circumferential pulmonary vein isolation of atrial fibrillation. *J Cardiovasc Electrophysiol* 2013;**24**:975–83.

46. Vogler J, Willems S, Sultan A, Schreiber D, Luker J, Servatius H *et al.* Pulmonary vein isolation versus defragmentation: the CHASE-AF clinical trial. *J Am Coll Cardiol* 2015;**66**:2743–52.

47. Calkins H, Hindricks G, Cappato R, Kim YH, Saad EB, Aguinaga L *et al.* 2017 HRS/EHRA/ECAS/APHRS/SOLAECE expert consensus statement on catheter and surgical ablation of atrial fibrillation. *Europace* 2018;**20**:e1–e160.

48. Grace A, Verma A, Willems S. Dipole density mapping of atrial fibrillation. *Eur Heart J* 2017;**38**:5–9.

49. Grace A, Willems S, Meyer C, Verma A, Heck P, Zhu M *et al.* High-resolution noncontact charge-density mapping of endocardial activation. *JCI Insight* 2019;**4**:e126422.

50. Shi R, Parikh P, Chen Z, Angel N, Norman M, Hussain W *et al.* Validation of dipole density mapping during atrial fibrillation and sinus rhythm in human left atrium. *JACC Clin Electrophysiol* 2020;**6**:171–81.

51. Earley MJ, Abrams DJ, Sporton SC, Schilling RJ. Validation of the noncontact mapping system in the left atrium during permanent atrial fibrillation and sinus rhythm. *J Am Coll Cardiol* 2006;**48**:485–91.

52. Allessie MA, Bonke FI, Schopman FJ. Circus movement in rabbit atrial muscle as a mechanism of tachycardia. III. The "leading circle" concept: a new model of circus movement in cardiac tissue without the involvement of an anatomical obstacle. *Circ Res* 1977;**41**:9–18.

53. Kuklik P, Zeemering S, Maesen B, Maessen J, Crijns HJ, Verheule S *et al.* Reconstruction of instantaneous phase of unipolar atrial contact electrogram using a concept of sinusoidal recomposition and Hilbert transform. *IEEE Trans Biomed Eng* 2015;**62**:296–302.

54. Jalife J, Berenfeld O, Mansour M. Mother rotors and fibrillatory conduction: a mechanism of atrial fibrillation. *Cardiovasc Res* 2002;**54**:204–16.

55. Roney CH, Cantwell CD, Qureshi NA, Chowdhury RA, Dupont E, Lim PB *et al.* Rotor tracking using phase of electrograms recorded during atrial fibrillation. *Ann Biomed Eng* 2017;**45**:910–23.

56. Berenfeld O, Oral H. The quest for rotors in atrial fibrillation: different nets catch different fishes. *Heart Rhythm* 2012;**9**:1440–1.

57. Haissaguerre M, Hocini M, Denis A, Shah AJ, Komatsu Y, Yamashita S *et al.* Driver domains in persistent atrial fibrillation. *Circulation* 2014;**130**:530–8.

58. Swarup V, Baykaner T, Rostamian A, Daubert JP, Hummel J, Krummen DE *et al.* Stability of rotors and focal sources for human atrial fibrillation: focal impulse and rotor mapping (FIRM) of AF sources and fibrillatory conduction. *J Cardiovasc Electrophysiol* 2014;**25**:1284–92.

59. Ravelli F, Mase M. Computational mapping in atrial fibrillation: how the integration of signal-derived maps may guide the localization of critical sources. *Europace* 2014;**16**:714–23.

60. Botteron GW, Smith JM. A technique for measurement of the extent of spatial organization of atrial activation during atrial fibrillation in the intact human heart. *IEEE Trans Biomed Eng* 1995;**42**:579–86.

61. Castells F, Cervigon R, Millet J. On the preprocessing of atrial electrograms in atrial fibrillation: understanding Botteron's approach. *Pacing Clin Electrophysiol* 2014;**37**:133–43.

62. Everett THt, Kok LC, Vaughn RH, Moorman JR, Haines DE. Frequency domain algorithm for quantifying atrial fibrillation organization to increase defibrillation efficacy. *IEEE Trans Biomed Eng* 2001;**48**:969–78.

63. Lin YJ, Tsao HM, Chang SL, Lo LW, Hu YF, Chang CJ *et al.* Role of high dominant frequency sites in nonparoxysmal atrial fibrillation patients: insights from high-density frequency and fractionation mapping. *Heart Rhythm* 2010;**7**:1255–62.

64. Gadenz L, Hashemi J, Shariat MH, Gula L, Redfearn DP. Clinical role of dominant frequency measurements in atrial fibrillation ablation—a systematic review. *J Atr Fibrillation* 2017;**9**:1548.

65. Verma A, Lakkireddy D, Wulffhart Z, Pillarisetti J, Farina D, Beardsall M *et al.* Relationship between complex fractionated electrograms (CFE) and dominant frequency (DF) sites and prospective assessment of adding DF-guided ablation to pulmonary vein isolation in persistent atrial fibrillation (AF). *J Cardiovasc Electrophysiol* 2011;**22**:1309–16.

66. Atienza F, Almendral J, Jalife J, Zlochiver S, Ploutz-Snyder R, Torrecilla EG *et al.* Real-time dominant frequency mapping and ablation of dominant frequency sites in atrial fibrillation with left-to-right frequency gradients predicts long-term maintenance of sinus rhythm. *Heart Rhythm* 2009;**6**:33–40.

67. Atienza F, Almendral J, Ormaetxe JM, Moya A, Martinez-Alday JD, Hernandez-Madrid A *et al.*; RADAR-AF Investigators. Comparison of radiofrequency catheter ablation of drivers and circumferential pulmonary vein isolation in atrial fibrillation: a noninferiority randomized multicenter RADAR-AF trial. *J Am Coll Cardiol* 2014;**64**:2455–67.

68. Weber FM, Schilling C, Seemann G, Luik A, Schmitt C, Lorenz C *et al.* Wave-direction and conduction-velocity analysis from intracardiac electrograms–a single-shot technique. *IEEE Trans Biomed Eng* 2010;**57**:2394–401.

69. Anter E, Duytschaever M, Shen CY, Strisciuglio T, Leshem E, Contreras-Valdes FM *et al.* Activation mapping with integration of vector and velocity information improves the ability to identify the mechanism and location of complex scar-related atrial tachycardias. *Circ Arrhythmia Electrophysiol* 2018;**11**.

70. Dallet C, Roney C, Martin R, Kitamura T, Puyo S, Duchateau J et al. Cardiac propagation pattern mapping with vector field for helping tachyarrhythmias diagnosis with clinical tridimensional electro-anatomical mapping tools. *IEEE Trans Biomed Eng* 2019;**66**:373–82.

71. Coveney S, Corrado C, Roney CH, Wilkinson RD, Oakley JE, Lindgren F et al. Probabilistic interpolation of uncertain local activation times on human atrial manifolds. *IEEE Trans Biomed Eng* 2020;**67**:99–109.

72. van Schie MS, Starreveld R, Bogers A, de Groot NMS. Sinus rhythm voltage fingerprinting in patients with mitral valve disease using a high-density epicardial mapping approach. *Europace* 2021;**23**:469–78.

73. Ganesan AN, Kuklik P, Lau DH, Brooks AG, Baumert M, Lim WW et al. Bipolar electrogram shannon entropy at sites of rotational activation implications for ablation of atrial fibrillation. *Circ Arrhythm Electrophysiol* 2013;**6**:48–57.

74. Cuculich PS, Wang Y, Lindsay BD, Faddis MN, Schuessler RB, Damiano RJ Jr. et al. Noninvasive characterization of epicardial activation in humans with diverse atrial fibrillation patterns. *Circulation* 2010;**122**:1364–72.

75. Shah AJ, Hocini M, Xhaet O, Pascale P, Roten L, Wilton SB et al. Validation of novel 3-dimensional electrocardiographic mapping of atrial tachycardias by invasive mapping and ablation: a multicenter study. *J Am Coll Cardiol* 2013;**62**: 889–97.

76. Salinet J, Molero R, Schlindwein FS, Karel J, Rodrigo M, Rojo-Álvarez JL et al. Electrocardiographic imaging for atrial fibrillation: a perspective from computer models and animal experiments to clinical value. *Front Physiol* 2021;**12**:653013.

77. Ramanathan C, Ghanem RN, Jia P, Ryu K, Rudy Y. Noninvasive electrocardiographic imaging for cardiac electrophysiology and arrhythmia. *Nat Med* 2004;**10**: 422–8.

78. Bear LR, LeGrice IJ, Sands GB, Lever NA, Loiselle DS, Paterson DJ et al. How accurate is inverse electrocardiographic mapping? a systematic in vivo evaluation. *Circ Arrhythm Electrophysiol* 2018;**11**:e006108.

79. Duchateau J, Sacher F, Pambrun T, Derval N, Chamorro-Servent J, Denis A et al. Performance and limitations of noninvasive cardiac activation mapping. *Heart Rhythm* 2019;**16**:435–42.

80. Dubois R, Shah AJ, Hocini M, Denis A, Derval N, Cochet H et al. Non-invasive cardiac mapping in clinical practice: application to the ablation of cardiac arrhythmias. *J Electrocardiol* 2015;**48**:966–74.

81. Schuler S, Potyagaylo D, Dossel O. ECG imaging of simulated atrial fibrillation: imposing epi-endocardial similarity facilitates the reconstruction of transmembrane voltages. *Comput Cardiol* 2017;**44**: 245–303.

82. Boyle PM, Hakim JB, Zahid S, Franceschi WH, Murphy MJ, Vigmond EJ et al. Comparing reentrant drivers predicted by image-based computational modeling and mapped by electrocardiographic imaging in persistent atrial fibrillation. *Front Physiol* 2018;**9**:414.

83. Haissaguerre M, Hocini M, Shah AJ, Derval N, Sacher F, Jais P et al. Noninvasive panoramic mapping of human atrial fibrillation mechanisms: a feasibility report. *J Cardiovasc Electrophysiol* 2013;**24**:711–7.

84. Vijayakumar R, Vasireddi SK, Cuculich PS, Faddis MN, Rudy Y. Methodology considerations in phase mapping of human cardiac arrhythmias. *Circ Arrhythm Electrophysiol* 2016;**9**:e004409.

85. Coll-Font J, Dhamala J, Potyagaylo D, Schulze WH, Tate JD, Guillem MS et al. The consortium for electrocardiographic imaging. *Comput Cardiol* 2016;**43**: 325–8.

86. Sirish P, Li N, Timofeyev V, Zhang XD, Wang L, Yang J et al. Molecular mechanisms and new treatment paradigm for atrial fibrillation. *Circ Arrhythm Electrophysiol* 2016;**9**:e003721.

87. Nyns ECA, Poelma RH, Volkers L, Plomp JJ, Bart CI, Kip AM et al. An automated hybrid bioelectronic system for autogenous restoration of sinus rhythm in atrial fibrillation. *Sci Transl Med* 2019;**11**:eaau6447.

88. Polina I, Jansen HJ, Li T, Moghtadaei M, Bohne LJ, Liu Y et al. Loss of insulin signaling may contribute to atrial fibrillation and atrial electrical remodeling in type 1 diabetes. *Proc Natl Acad Sci USA* 2020;**117**:7990–8000.

89. Hansen BJ, Zhao J, Li N, Zolotarev A, Zakharkin S, Wang Y et al. Human atrial fibrillation drivers resolved with integrated functional and structural imaging to benefit clinical mapping. *JACC Clin Electrophysiol* 2018;**4**:1501–15.

90. Boyle PM, Zghaib T, Zahid S, Ali RL, Deng D, Franceschi WH et al. Computationally guided personalized targeted ablation of persistent atrial fibrillation. *Nat Biomed Eng* 2019;**3**:870–9.

91. Zhao J, Hansen BJ, Wang Y, Csepe TA, Sul LV, Tang A et al. Three-dimensional Integrated functional, structural, and computational mapping to define the structural "Fingerprints" of heart-specific atrial fibrillation drivers in human heart ex vivo. *J Am Heart Assoc* 2017;**6**:e003721.

92. Lee P, Calvo CJ, Alfonso-Almazan JM, Quintanilla JG, Chorro FJ, Yan P et al. Low-cost optical mapping systems for panoramic imaging of complex arrhythmias and drug-action in translational heart models. *Sci Rep* 2017;**7**:43217.

93. Gloschat C, Aras K, Gupta S, Faye NR, Zhang H, Syunyaev RA et al. RHYTHM: an open source imaging toolkit for cardiac panoramic optical mapping. *Sci Rep* 2018;**8**:2921.

94. Kappadan V, Telele S, Uzelac I, Fenton F, Parlitz U, Luther S et al. High-resolution optical measurement of cardiac restitution, contraction, and fibrillation dynamics in beating vs. blebbistatin-uncoupled isolated rabbit hearts. *Front Physiol* 2020;**11**:464.

95. Lee S, Sahadevan J, Khrestian CM, Markowitz A, Waldo AL. Characterization of foci and breakthrough sites during persistent and long-standing persistent atrial fibrillation in patients: studies using high-density (510-512 Electrodes) biatrial epicardial mapping. *J Am Heart Assoc* 2017;**6**:e005274.

96. Teuwen CP, Yaksh A, Lanters EA, Kik C, van der Does LJ, Knops P et al. Relevance of conduction disorders in Bachmann's bundle during sinus rhythm in humans. *Circ Arrhythm Electrophysiol* 2016;**9**:e003972.

97. Hindricks G, Taborsky M, Glikson M, Heinrich U, Schumacher B, Katz A et al.; IN-TIME study group. Implant-based multiparameter telemonitoring of patients with heart failure (IN-TIME): a randomised controlled trial. *Lancet* 2014;**384**: 583–90.

98. Kohno R, Abe H, Oginosawa Y, Tamura M, Takeuchi M, Nagatomo T et al. Reliability and characteristics of atrial tachyarrhythmias detection in dual chamber pacemakers. *Circ J* 2011;**75**:1090–7.

99. Sanna T, Diener HC, Passman RS, Di Lazzaro V, Bernstein RA, Morillo CA et al. Cryptogenic stroke and underlying atrial fibrillation. *N Engl J Med* 2014;**370**: 2478–86.

100. Hanke T, Charitos EI, Stierle U, Karluss A, Kraatz E, Graf B et al. Twenty-four-hour holter monitor follow-up does not provide accurate heart rhythm status after surgical atrial fibrillation ablation therapy: up to 12 months experience with a novel permanently implantable heart rhythm monitor device. *Circulation* 2009;**120**:S177–184.

101. Verma A, Champagne J, Sapp J, Essebag V, Novak P, Skanes A et al. Discerning the incidence of symptomatic and asymptomatic episodes of atrial fibrillation before and after catheter ablation (DISCERN AF): a prospective, multicenter study. *JAMA Intern Med* 2013;**173**:149–56.

102. Kapa S, Epstein AE, Callans DJ, Garcia FC, Lin D, Bala R et al. Assessing arrhythmia burden after catheter ablation of atrial fibrillation using an implantable loop recorder: the ABACUS study. *J Cardiovasc Electrophysiol* 2013;**24**:875–81.

103. Pokushalov E, Romanov A, Corbucci G, Artyomenko S, Turov A, Shirokova N et al. Use of an implantable monitor to detect arrhythmia recurrences and select patients for early repeat catheter ablation for atrial fibrillation: a pilot study. *Circ Arrhythm Electrophysiol* 2011;**4**:823–31.

104. Platonov PG, Stridh M, de Melis M, Urban L, Carlson J, Corbucci G et al. Analysis of atrial fibrillatory rate during spontaneous episodes of atrial fibrillation in humans using implantable loop recorder electrocardiogram. *J Electrocardiol* 2012;**45**:723–6.

105. Hindricks G, Pokushalov E, Urban L, Taborsky M, Kuck KH, Lebedev D et al.; XPECT Trial Investigators. Performance of a new leadless implantable cardiac monitor in detecting and quantifying atrial fibrillation: results of the XPECT trial. *Circ Arrhythm Electrophysiol* 2010;**3**:141–7.

106. Nölker G, Mayer J, Boldt L-H, Seidl K, VAN Driel V, Massa T et al. Performance of an Implantable cardiac monitor to detect atrial fibrillation: results of the DETECT AF study. *J Cardiovasc Electrophysiol* 2016;**27**:1403–10.

107. Purerfellner H, Pokushalov E, Sarkar S, Koehler J, Zhou R, Urban L et al. P-wave evidence as a method for improving algorithm to detect atrial fibrillation in insertable cardiac monitors. *Heart Rhythm* 2014;**11**:1575–83.

108. Sanders P, Purerfellner H, Pokushalov E, Sarkar S, Di Bacco M, Maus B et al.; Reveal LINQ Usability Investigators. Performance of a new atrial fibrillation detection algorithm in a miniaturized insertable cardiac monitor: results from the reveal LINQ usability study. *Heart Rhythm* 2016;**13**:1425–30.

109. Mariani JA, Weerasooriya R, van den Brink O, Mohamed U, Gould PA, Pathak RK et al. Miniaturized implantable cardiac monitor with a long sensing vector (BIOMONITOR III): insertion procedure assessment, sensing performance, and home monitoring transmission success. *J Electrocardiol* 2020;**60**:118–25.

110. Purerfellner H, Sanders P, Sarkar S, Reisfeld E, Reiland J, Koehler J et al. Adapting detection sensitivity based on evidence of irregular sinus arrhythmia to improve atrial fibrillation detection in insertable cardiac monitors. *Europace* 2018;**20**:f321–f328.

111. Ciconte G, Saviano M, Giannelli L, Calovic Z, Baldi M, Ciaccio C et al. Atrial fibrillation detection using a novel three-vector cardiac implantable monitor: the atrial fibrillation detect study. *Europace* 2017;**19**:1101–8.

112. Schilling C, Keller M, Scherr D, Oesterlein T, Haissaguerre M, Schmitt C et al. Fuzzy decision tree to classify complex fractionated atrial electrograms. *Biomed Tech* 2015;**60**:245–55.

113. Reich C, Oesterlein T, Rottmann M, Seemann G, Dössel O. Classification of cardiac excitation patterns during atrial fibrillation. *Curr Dir Biomed Eng* 2016;**2**: 161–166.

114. Attia ZI, Noseworthy PA, Lopez-Jimenez F, Asirvatham SJ, Deshmukh AJ, Gersh BJ et al. An artificial intelligence-enabled ECG algorithm for the identification of patients with atrial fibrillation during sinus rhythm: a retrospective analysis of outcome prediction. *Lancet* 2019;**394**:861–7.

115. Mairesse GH, Moran P, Van Gelder IC, Elsner C, Rosenqvist M, Mant J *et al.*; ESC Scientific Document Group. Screening for atrial fibrillation: a European Heart Rhythm Association (EHRA) consensus document endorsed by the Heart Rhythm Society (HRS), Asia Pacific Heart Rhythm Society (APHRS), and Sociedad Latinoamericana de Estimulacion Cardiaca y Electrofisiologia (SOLAECE). *Europace* 2017;**19**:1589–623.

116. Varma N, Cygankiewicz I, Turakhia MP, Heidbuchel H, Hu YF, Chen LY *et al.* 2021 ISHNE/HRS/EHRA/APHRS expert collaborative statement on mhealth in arrhythmia management: digital medical tools for heart rhythm professionals: from the International Society for Holter and Noninvasive Electrocardiology/ Heart Rhythm Society/European Heart Rhythm Association/Asia-Pacific Heart Rhythm Society. *Circ Arrhythm Electrophysiol* 2021;**14**:e009204.

117. Budzianowski J, Hiczkiewicz J, Burchardt P, Pieszko K, Rzeźniczak J, Budzianowski P *et al.* Predictors of atrial fibrillation early recurrence following cryoballoon ablation of pulmonary veins using statistical assessment and machine learning algorithms. *Heart Vessels* 2019;**34**:352–9.

118. Furui K, Morishima I, Morita Y, Kanzaki Y, Takagi K, Yoshida R *et al.* Predicting long-term freedom from atrial fibrillation after catheter ablation by a machine learning algorithm: validation of the CAAP-AF score. *J Arrhythm* 2020;**36**: 297–303.

119. Hung M, Hon ES, Lauren E, Xu J, Judd G, Su W. Machine learning approach to predict risk of 90-day hospital readmissions in patients with atrial fibrillation: implications for quality improvement in healthcare. *Health Serv Res Manag Epidemiol* 2020;**7**:2333392820961887.

120. Hung M, Lauren E, Hon E, Xu J, Ruiz-Negron B, Rosales M *et al.* Using machine learning to predict 30-day hospital readmissions in patients with atrial fibrillation undergoing catheter ablation. *J Pers Med* 2020;**10**:jpm10030082.

121. Li W, Lipsky MS, Hon ES, Su W, Su S, He Y *et al.* Predicting all-cause 90-day hospital readmission for dental patients using machine learning methods. *BDJ Open* 2021;**7**:1.

122. Alhusseini MI, Abuzaid F, Rogers AJ, Zaman JAB, Baykaner T, Clopton P *et al.* Machine learning to classify intracardiac electrical patterns during atrial fibrillation: machine learning of atrial fibrillation. *Circ Arrhythm Electrophysiol* 2020;**13**: e008160.

123. Shade JK, Ali RL, Basile D, Popescu D, Akhtar T, Marine JE *et al.* Preprocedure application of machine learning and mechanistic simulations predicts likelihood of paroxysmal atrial fibrillation recurrence following pulmonary vein isolation. *Circ Arrhythm Electrophysiol* 2020;**13**:e008213.